

# RESONANCE AT 125 GeV: HIGGS OR DILATON/RADION?

Zackaria Chacko <sup>\*</sup>, Roberto Franceschini <sup>†</sup>, and Rashmish K. Mishra <sup>‡</sup>

Maryland Center for Fundamental Physics, Department of Physics,  
University of Maryland, College Park, MD 20742, USA

## Abstract

We consider the possibility that the new particle that has been observed at 125 GeV is not the Standard Model (SM) Higgs, but instead the dilaton associated with an approximate conformal symmetry that has been spontaneously broken. We focus on dilatons that arise from theories of technicolor, or from theories of the Higgs as a pseudo-Nambu-Goldstone boson (pNGB), that involve strong conformal dynamics in the ultraviolet. In the pNGB case, we are considering a framework where the Higgs particle is significantly heavier than the dilaton and has therefore not yet been observed. In each of the technicolor and pNGB scenarios, we study both the case when the SM fermions and gauge bosons are elementary, and the case when they are composites of the strongly interacting sector. Our analysis incorporates conformal symmetry violating effects, which are necessarily present since the dilaton is not massless, and is directly applicable to a broad class of models that stabilize the weak scale and involve strong conformal dynamics. Since the AdS/CFT correspondence relates the radion in Randall-Sundrum (RS) models to the dilaton, our results also apply to RS models with the SM fields localized on the infrared brane, or in the bulk. We identify the parameters that can be used to distinguish the dilatons associated with the several different classes of theories being considered from each other, and from the SM Higgs. We perform a fit to all the available data from several experiments and highlight the key observations to extract these parameters. We find that at present, both the technicolor and pNGB dilaton scenarios provide a good fit to the data, comparable to the SM Higgs. We indicate the future observations that will help to corroborate or falsify each scenario.

---

<sup>\*</sup>[zchacko@umd.edu](mailto:zchacko@umd.edu)

<sup>†</sup>[rfrances@umd.edu](mailto:rfrances@umd.edu)

<sup>‡</sup>[rashmish@umd.edu](mailto:rashmish@umd.edu)

# 1 Introduction

The Large Hadron Collider (LHC) is currently well on its way to uncovering the mechanism that underlies the breaking of electroweak symmetry. The discovery of a Higgs-like particle localized at a mass of about 125 GeV by ATLAS and CMS [1, 2] is just the first step towards a thorough understanding of the phenomenon of electroweak symmetry breaking (EWSB).

The resonance observed at the LHC sits at a rather special spot for experiment. In particular, the decays of a SM Higgs boson with such a mass have sizable branching fractions into several final states including  $b\bar{b}$ ,  $W^+W^-$ ,  $\tau\bar{\tau}$ ,  $ZZ$  and  $\gamma\gamma$ . Searching for signals of the new particle, produced either singly or in association with  $W$  bosons,  $Z$  bosons or well separated forward energetic jets, the LHC experiments expect to be able to measure with significant accuracy its branching ratios into each of these final states. These measurements will either confirm that the new state is the SM Higgs, or expose it as an impostor.

The availability of this data, and the presence of excesses above the expected background in several different channels (even above the SM Higgs signal hypothesis in some cases), has already motivated several analyses that undertake a global interpretation of the properties of the particle responsible for the new physics observed by ATLAS and CMS [3, 4, 5, 6, 7, 8, 9, 10, 11, 12, 13, 14, 15, 16, 17]. Although constrained by the limited luminosity, these global analyses have yielded several interesting results. In particular, it has been shown that the 2011 data disfavors a fermio-phobic Higgs boson [18, 19], and limits have been placed on the invisible decay width of the Higgs [6, 20, 21]. Furthermore these efforts have led to a productive discussion among theorists and experimentalists about the way to present the results of experimental searches. As detailed in Refs. [22, 23] some searches could potentially have a wider reach in terms of physics scenarios that are probed. The wish would be to see the analyses of inclusive and exclusive final states presented in a broad manner, as opposed to the (overly) tuned analysis

performed so far in most cases

On the theoretical side, 125 GeV is also a rather special value for the SM Higgs boson mass. Such a value of the Higgs mass is in the far periphery of the preferred parameter space of the Minimal Supersymmetric Standard Model (MSSM), and motivates the study of alternatives to supersymmetry that stabilize the weak scale. Several well-motivated models of electroweak symmetry breaking that solve the hierarchy problem involve strong conformal dynamics above the weak scale. In particular, in models of technicolor [24, 25], for a review see [26], and of the Higgs as a pseudo-Nambu-Goldstone boson (pNGB) [27, 28, 29, 30, 31], strong conformal dynamics can help separate the flavor scale from the weak scale [32], (see also [33, 34, 35, 36, 37]), allowing the bounds on flavor-changing neutral currents to be satisfied.

In theories where conformal symmetry is spontaneously broken, the low energy effective theory contains a massless scalar, the dilaton, which may be thought of as the Nambu-Goldstone boson (NGB) associated with the breaking of conformal symmetry [38, 39, 40, 41]. The form of the dilaton couplings is fixed by the requirement that conformal symmetry be realized non-linearly, and so this framework is extremely predictive. Several authors have studied the self-interactions of a light dilaton, and its couplings to SM fields [42, 43, 44, 45]. Interestingly, the couplings of a dilaton to the SM gauge and matter fields are very similar to those of a SM Higgs [43]. The reason is that at the classical level the SM has an approximate conformal symmetry which is violated only by the Higgs mass term. Since the VEV of the Higgs doublet spontaneously breaks this approximate conformal symmetry, in the classical limit the couplings of the Higgs to the SM fields are very similar to those of a dilaton. It is therefore very natural to ask the question whether the resonance observed by the LHC at 125 GeV could be the dilaton associated with a strongly interacting conformal sector that breaks electroweak symmetry, rather than the SM Higgs. This is the question we shall

focus on in this paper.

The remarkable fact that a dilaton can naturally mimic the SM Higgs boson has already lead to significant interest in the problem of distinguishing the two at colliders [43, 46, 47, 48, 49, 50, 51]. As such it is not surprising that the idea that the new physics behind the 125 GeV resonance could be the dilaton (in combination or not with a Higgs boson) has already been put forward [52, 53, 54, 55, 56, 57, 58], [6, 7, 10, 11, 12, 13, 14]. However the types of dilaton that have been considered so far in the post-LHC literature are rather specific, and the analyses do not apply to many of the theories that are of primary interest for electroweak symmetry breaking. Furthermore, these studies do not include the effects of conformal symmetry violation, which is necessarily present since the dilaton is not massless, and can sometimes be significant. Our analysis extends to more general incarnations of the dilaton, incorporates conformal symmetry violating effects, and is directly applicable to a broad class of models that stabilize the weak scale and involve strong conformal dynamics.

Specifically we consider the possibility that the new particle that has been observed at 125 GeV is a dilaton that arises from a theory of technicolor, or from a theory of the Higgs as a pNGB, that involves strong conformal dynamics in the ultraviolet. In the pNGB case, we are considering a framework where the Higgs particle is significantly heavier than the dilaton and has therefore not yet been observed. In each of the technicolor and pNGB scenarios, we study both the case when the SM fermions and gauge bosons are elementary, and the case when they are composites of the strongly interacting sector. We identify the parameters that can be used to distinguish the dilatons associated with the several different classes of theories being considered from each other, and from the SM Higgs. We perform a fit to all the available data from several experiments and highlight the key observations to extract these parameters. We also indicate the future observations that should help to corroborate or falsify each scenario.

The AdS/CFT correspondence [59, 60, 61, 62] relates Randall-Sundrum (RS)

models in warped extra dimensions [63] to strongly coupled conformal field theories in the large  $N$  limit. In this way, extra dimensional realizations of technicolor [64] and of the Higgs as a pNGB [65, 66] have been obtained. In the correspondence, the radion in the RS model is identified with the dilaton [42]. The couplings of the radion to the SM gauge and matter fields have been studied, both in the case when the SM fields are localized to the infrared brane [67, 68, 69, 70, 71] and in the case when they are in the bulk [72, 73], and agree with the dilaton couplings in the appropriate limit. Our results on the dilaton therefore also apply to the radion in RS models, with the SM fields localized on the brane, or in the bulk.

## 2 Interactions of the dilaton

### 2.1 General Considerations

The fifteen parameter conformal group includes scale transformations and special conformal transformations, in addition to the ten parameters of the Poincare group. If conformal invariance is spontaneously broken the low energy effective theory contains a massless dilaton field  $\sigma(x)$ , which can be thought of as the NGB associated with the breaking of scale invariance [38, 39, 40, 41, 74, 75]. The additional four NGBs associated with the breaking of the special conformal symmetry can be identified with the derivatives of the dilaton, rather than as independent dynamical fields. Below the breaking scale the symmetry is realized non-linearly, with the dilaton undergoing a shift  $\sigma(x) \rightarrow \sigma'(x') = \sigma(x) + \omega f$  under the scale transformation  $x^\mu \rightarrow x'^\mu = e^{-\omega} x^\mu$ . Here  $f$  is the scale associated with the breaking of conformal symmetry. For the purpose of writing interactions of the dilaton it is convenient to define the conformal compensator

$$\chi(x) = f e^{\sigma(x)/f} \tag{1}$$

which transforms linearly under scale transformations. Specifically, under the scale transformation  $x^\mu \rightarrow x'^\mu = e^{-\omega} x^\mu$ ,  $\chi(x)$  transforms as

$$\chi(x) \rightarrow \chi'(x') = e^\omega \chi(x). \quad (2)$$

The low energy effective theory for the dilaton will in general include all terms consistent with this transformation, but with some additional restrictions on their coefficients from the requirement that the theory be invariant not just under scale transformations, but under the full conformal group. These restrictions will not affect our discussion in any significant way, and so in practice we shall only require that the action for  $\chi$  be scale invariant.

In realistic models of electroweak symmetry breaking conformal symmetry is not exact. As a consequence the dilaton will acquire a mass, and there will be corrections to its couplings from conformal symmetry violating effects. If the dimension of the operator responsible for the breaking of conformal symmetry is close to marginal even at the breaking scale, the mass of the dilaton can naturally lie below the scale of strong dynamics [76, 45], see also [77]. Although this condition is, in general, not satisfied in the scenarios of interest for electroweak symmetry breaking, the presence of a light dilaton in these theories is only associated with mild tuning [45]. This makes it a priori quite plausible that the Higgs-like particle observed at the LHC is in fact a dilaton. Corrections to the form of the dilaton couplings to SM states from the conformal symmetry violating effects that generate the dilaton mass are suppressed by the square of the ratio of the dilaton mass to the strong coupling scale [45]. Although this is a small parameter in the theories of interest, corrections to the couplings can nevertheless sometimes be significant and will need to be taken into account in our analysis.

The strength of the dilaton couplings is controlled by the parameter  $f$ , the scale at which conformal symmetry is broken. In technicolor models, the same condensate that breaks electroweak symmetry also breaks conformal symmetry.

Hence we expect that  $f$  is of order the electroweak VEV,  $v$ , in theories of technicolor. For models of the Higgs as a pNGB, however, the situation is different. It is the same dynamics that breaks the global symmetry of which the Higgs is a pNGB that now breaks conformal symmetry. Then, depending on the scale at which the global symmetry is broken, there can be a hierarchy between  $v$  and  $f$ . Since precision electroweak measurements prefer the Higgs compositeness scale  $\Lambda \sim 4\pi f$  to be 5 TeV or larger, the favored values of  $f$  are such that  $f \gtrsim 3v$ .

We introduce the variable

$$\xi = \frac{v^2}{f^2}$$

to parametrize the ratio of breaking scales. Technicolor theories are associated with values of  $\xi$  close to one. Meanwhile  $\xi = 0$  describes a pNGB-like model with the cutoff pushed very high, corresponding to the SM-like limit of these theories. In this limit, the pNGB scenario is highly tuned and completely fails as a solution to the hierarchy problem. On the other hand precision electroweak measurements prefer the Higgs compositeness scale  $\Lambda \sim 4\pi f$  to be 5 TeV or larger. As such a moderate  $\xi$  is expected in pNGB models to solve the hierarchy problem and not be in tension with precision tests.

## 2.2 Dilaton couplings to the SM Fields

The next step is to understand the dilaton couplings to the SM fields. Mixing between the dilaton and a pNGB Higgs is generally small, particularly if  $v \ll f$  or if the dilaton is significantly lighter than the Higgs (or vice versa). We shall therefore neglect it. The form of the dilaton couplings to the SM fermions and gauge bosons is then the same in the technicolor and pNGB cases [45].

We will consider in turn the dilaton couplings to massive gauge bosons, massless gauge bosons and fermions. The form of these interactions depends on whether the SM fields are elementary particles or composites of the strongly interacting sector, and we will consider both possibilities. The AdS/CFT cor-

respondence relates composite fermions and gauge bosons to states localized on or towards the infrared brane in RS models. Elementary fermions are associated with states localized towards the ultraviolet brane and elementary gauge bosons live in the bulk of the space. The radion couplings to brane and bulk fields in RS models can therefore be determined from the corresponding interactions of the dilaton. Our results for the dilaton are therefore directly applicable to the radion in certain classes of RS models. However, in our analysis we will not consider constraints on the parameters of the RS model arising from limits on other particles in the spectrum, such as Kaluza-Klein excitations of the graviton, (see for example [79, 78]).

### 2.2.1 Dilaton couplings to the massive gauge bosons

Depending on the model, the massive gauge bosons of the SM, the  $W$  and  $Z$ , could either be elementary particles or composite states that emerge at low energies from the strong conformal dynamics. In either case the gauge boson mass term

$$\frac{m_W^2}{g^2} W^2$$

is the leading effect which breaks conformal symmetry. Then the dilaton couples in such a way as to compensate for this [43, 45],

$$\frac{\chi^2}{f^2} \frac{m_W^2}{g^2} W^2 \rightarrow 2 \frac{\sigma}{f} \frac{m_W^2}{g^2} W^2.$$

Note that we are working in a basis where the gauge boson kinetic terms have the form

$$-\frac{1}{4g^2} F_{\mu\nu} F^{\mu\nu}.$$

We see that the coupling of the dilaton is in general suppressed by a factor  $\frac{v}{f} = \sqrt{\xi}$  with respect to the coupling of a SM Higgs boson. Corrections to the form of this interaction from conformal symmetry violating effects are small [45].



### 2.2.2 Dilaton coupling to the massless gauge bosons

In the case of the massless gauge bosons, the photon and the gluon, there is no classical source of breaking of the conformal symmetry. However, at the quantum level conformal invariance is broken, as manifested by the renormalization group evolution of the gauge couplings

$$\frac{d}{d \log \mu} \frac{1}{g^2} = \frac{b}{8\pi^2}.$$

The dilaton couples in such a way as to compensate for this effect. The form of this coupling depends on whether the gauge bosons are elementary particles or composites of the conformal field theory.

Let us consider first the case when the photon and gluon are elementary. Then the evolution of the gauge couplings is different above and below the strong coupling scale  $\Lambda \sim 4\pi f$ . We parametrize the running of the gauge couplings above and below  $\Lambda$  by  $b_>$  and  $b_<$  respectively. Above the top mass,  $b_< = +7$  for the gluon and  $-11/3$  for the photon. The running of the gauge couplings above the scale  $\Lambda$  constitutes an explicit, rather than spontaneous, breaking of conformal symmetry. A spurion analysis then shows that the dilaton couples to elementary massless gauge bosons as [45]

$$\frac{1}{32\pi^2} (b_< - b_>) \frac{\sigma}{f} F_{\mu\nu} F^{\mu\nu}. \quad (3)$$

This formula is valid at scales slightly below the strong coupling scale  $4\pi f$ . Corrections from the conformal symmetry violating effects that generate the dilaton mass are again small [45].

In the class of theories of interest the conformal sector necessarily transforms under electromagnetism. However in theories where the top quark is not composite, this sector need not be charged under the SM color group. Then  $b_> = b_<$  for SM color, and the leading coupling of the dilaton to the gluons arises from a

calculable top loop. In theories where the top quark is composite the conformal sector is necessarily charged under the SM color group. However, since the gluon is elementary,  $b_>$  is not constrained by conformal invariance, and its value depends on details of the specific conformal sector at hand. The difference  $b_> - b_<$  is associated with the number of states in the strongly interacting sector with masses of order  $\Lambda$ , and is expected to be of order a few.

In the case of composite gauge bosons, there is no explicit breaking of conformal symmetry above the scale  $\Lambda$ . As a consequence, the formula Eq. (3) still applies, but with  $b_> = 0$  [43]. Since  $b_<$  is known, it would appear that this framework is very predictive. However, in this scenario, corrections to the dilaton couplings from conformal symmetry violating effects can be significant. These take the form [45]

$$\frac{c}{4g^2} \frac{m_\sigma^2}{\Lambda^2} \frac{\sigma}{f} F_{\mu\nu} F^{\mu\nu},$$

where  $c$  is of order one. For  $\Lambda$  of order the TeV scale, and  $m_\sigma$  of order 100 GeV, this gives a contribution to the dilaton couplings comparable to Eq. (3), and predictivity is lost. This is particularly so in the case of the photon, less so for the gluon. For larger  $\Lambda \gtrsim 3$  TeV, these corrections are much smaller, and predictivity is restored. It follows from this that the couplings of the dilaton to massless gauge bosons, if composite, differ from those of the SM Higgs by the product of  $\sqrt{\xi}$  and a multiplicative factor of order a few. This factor can be predicted for larger values of  $\Lambda$ , but not for small  $\Lambda$ .

### 2.2.3 Dilaton couplings to the SM fermions

In the case of the SM fermions the leading source of conformal symmetry breaking are the fermion mass terms. The coupling of the dilaton depends on whether the SM fermions are purely elementary particles or are composites, or partial composites of the strong conformal dynamics.

In the case of elementary fermions their mass arises from direct couplings to a scalar operator  $\mathcal{H}$  in the conformal field theory with the gauge quantum numbers of the SM Higgs, as in theories of conformal technicolor [32]. For the third generation up-type quarks these couplings take the form

$$\mathcal{L} = y_{top} Q_3 \mathcal{H} t^c + h.c. .$$

This leads to the mass term for the top which we write as

$$m_t Q_3 t^c .$$

The condition that the flavor problem be addressed means that the large value of the top mass constrains the size of  $\Delta_{\mathcal{H}}$ . If we denote the flavor scale by  $\Lambda_F$ , we require

$$\left( \frac{\Lambda_F}{4\pi f} \right)^{\Delta_{\mathcal{H}}-1} \lesssim \frac{4\pi v}{m_t} .$$

For  $\Lambda_F \gtrsim 1000$  TeV, we require  $\Delta_{\mathcal{H}} \lesssim 1.3$  for the technicolor case. For the pNGB case, with  $f \sim 1$  TeV, the constraint becomes  $\Delta_{\mathcal{H}} \lesssim 1.5$ . At the same time, the hierarchy problem constrains the dimension of the operator  $\mathcal{H}^\dagger \mathcal{H}$  to be of order 4 or larger. Since  $\Delta_{\mathcal{H}} = 1$  necessarily implies that the conformal field theory is free, which in turn implies  $\Delta_{\mathcal{H}^\dagger \mathcal{H}} = 2$ , the conditions  $\Delta_{\mathcal{H}} \lesssim 1.3$  (or  $\Delta_{\mathcal{H}} \lesssim 1.5$ ) and  $\Delta_{\mathcal{H}^\dagger \mathcal{H}} \gtrsim 4$  are in tension. Note that these conditions cannot be simultaneously satisfied in the large  $N$  limit, and therefore realistic models of this type with elementary fermions cannot be constructed within the RS framework. Unitarity and causality can be used to constrain  $\Delta_{\mathcal{H}} \gtrsim 1.5$  if  $\Delta_{\mathcal{H}^\dagger \mathcal{H}} \gtrsim 4$  [80, 81, 82], [83], [84], (see also [85]). Therefore the technicolor scenario with elementary fermions is somewhat tuned.

A spurion analysis shows that the dilaton couples to the top quarks as [44, 45]

$$\frac{m_t}{f} \Delta_{\mathcal{H}} \sigma Q_3 t^c .$$

This differs by a factor of  $\sqrt{\xi}\Delta_{\mathcal{H}}$  from the top Yukawa coupling in the SM. More generally, the couplings of all the fermions to the dilaton will differ from that of the SM Higgs by this factor. Corrections to this expression from the conformal symmetry violating effects that lead to the dilaton mass are small [45].

From this discussion it is clear that a useful parametrization of the coupling of the dilaton to the top quark in the case of elementary fermions is as

$$\frac{m_t}{f} (1 + \epsilon) \sigma Q_3 t^c ,$$

where  $\epsilon = \Delta_{\mathcal{H}} - 1$ .

More generally, we can apply the same parametrization to the dilaton couplings with the other fermions as well, so that the interactions of the dilaton with elementary SM fermions differ from those of the Higgs by a universal factor of  $\sqrt{\xi}(1 + \epsilon)$ .

Another possibility is that the SM fermions are partially composite, emerging from the mixing of elementary fermions with operators in the conformal field theory that have the same gauge quantum numbers [86, 87]. For the up-type quarks this takes the form

$$\mathcal{L} = \tilde{y}_Q Q \mathcal{Q} + \tilde{y}_u u^c \mathcal{U} + h.c. . \tag{4}$$

Here  $\mathcal{Q}$  and  $\mathcal{U}$  are operators in the CFT with scaling dimension  $\Delta_Q$  and  $\Delta_u$ , respectively, and for simplicity we are suppressing flavor indices. The resulting mass term is of the form

$$m_u Q u^c ,$$

where  $m_u$  is proportional to the product  $\tilde{y}_Q \tilde{y}_u$  up to effects that are higher order

in  $y$ . A spurion analysis then show that the dilaton couples as [44, 45]

$$\frac{m_u}{f} (\Delta_Q + \Delta_u - 4) \sigma Q u^c .$$

We see that this coupling differs from that of the SM Higgs boson by the factor  $\frac{v}{f} (\Delta_Q + \Delta_u - 4)$ . Corrections from the conformal symmetry violating effects that generate the dilaton mass are small [45].

However, as in the case of elementary fermions, the scaling dimensions of the relevant operators are bound by phenomenological considerations. In fact to generate a large mass for the top quark we need  $\tilde{y}_Q$  and  $\tilde{y}_u$  for the third generation to be of order one at the scale  $\Lambda$ . For a high flavor scale  $\Lambda_F$ , in the absence of tuning, this implies that the terms in Eq. (4) that generate the top quark mass are close to marginal, corresponding to  $\Delta_Q \simeq 5/2$  and  $\Delta_u \simeq 5/2$ . As such in this scenario the deviation from the coupling of the SM Higgs is determined by the extent to which the terms in Eq. (4) deviate from exact marginality.

For  $\Delta_Q = \Delta_u = 5/2$ , the terms in Eq. (4) are exactly marginal and do not violate conformal symmetry. In this limit the coupling of the dilaton is suppressed simply by a factor of  $\sqrt{\xi} = v/f$  with respect to the coupling of the SM Higgs boson. Not surprisingly, the same result is obtained if the SM fermions  $Q$  and  $u^c$  are fully composite states, since in this limit the Yukawa coupling again arises from an effect that does not violate conformal symmetry.

For our analysis, the dilaton couplings to the third generation fermions are particularly important, since the current data is only sensitive to these interactions. For concreteness, in our analysis of partially composite fermions, we will set  $\Delta_Q = \Delta_u = 5/2$  for the top quark, corresponding to a fully composite top. More generally, we will assume that all the third generation SM fermions are primarily composite, so that their coupling to the dilaton is identical to that of the SM Higgs up to an overall factor of  $\sqrt{\xi}$ .

	<b>Elementary Fermions</b>	<b>Composite Fermions</b>
$\eta_{bb}$	$(\epsilon + 1)^2 \xi$	$\xi$
$\eta_{WW}$	$\xi$	$\xi$
$\eta_{\tau\tau}$	$(\epsilon + 1)^2 \xi$	$\xi$
$\eta_{ZZ}$	$\xi$	$\xi$
$\eta_{gg}$	$(\epsilon + 1)^2 \xi$	$\xi\psi$
$\eta_{\gamma\gamma}$	$\xi\phi$	$\xi\phi$

Table 1: Summary of the couplings of the dilaton.

### 3 Global fit of the Higgs data

#### 3.1 Couplings and relevant observables

In this section we summarize the couplings of the general dilaton introduced earlier, and identify the observables in the Higgs searches that are particularly sensitive to the parameters of the theory. We specifically focus on the three different classes of theories below:

- Theories where the SM fermions and gauge bosons are all elementary,
- Theories where the SM matter fields are composites of the strong dynamics, but the gauge fields are elementary.
- Theories where the SM matter and gauge fields are all composite.

For a more compact expression of the parametric behavior of the event rate we introduce the ratio of the square of the coupling of the dilaton to a given SM state over the square of the corresponding Higgs coupling in the SM,

$$\eta_{XX} \equiv \left( \frac{g_{\sigma XX}}{g_{hXX}} \right)^2.$$

The values of  $\eta$  at tree-level associated with the different SM states are shown in Table 1, both for the case when the third generation fermions are elementary

and the case when they are composite. In the scenario where the third generation fermions are composite, the SM gauge bosons could be either elementary or composite. We parametrize both cases the same way because the only significant difference in the analysis arises from the fact that if the SM gauge bosons are composite, then for larger values of  $f$ , corresponding to the range  $\xi \lesssim 1/10$ , the values of the parameters  $\phi$  and  $\psi$  are fixed.

We also remark that our parametrization of the couplings to massless vectors does not distinguish between calculable contributions of SM states and a priori unknown and largely unconstrained contributions arising from CFT states. This parametrization has the advantage of simplicity and can be easily mapped onto the predictions of specific UV scenarios. For instance in the case of composite gauge bosons the prediction would be:

$$\psi \simeq 132, \quad \phi \simeq 2.4. \tag{5}$$

It is also possible to parametrize the coupling to massless gauge bosons in a way that separates the SM and CFT contributions. Since the SM contribution can be calculated, an experimental determination of the dilaton couplings to the massless gauge bosons would in principle allow the possibility of measuring properties of the CFT (up to the remaining uncertainty on the SM part). Since our primary focus is on the issue of distinguishing the SM Higgs from the dilaton, we leave this for future work.

In what follows we consider in turn the scenarios with elementary fermions and composite fermions, and identify in each case the observations that will allow the parameters in Table 1 to be extracted.

### 3.1.1 Elementary Fermions

For elementary SM fermions the rate for the final state  $X\bar{X}$  in the case of a dilaton produced from gluons through a top loop is given by

$$\begin{aligned}
\sigma_{GF}^{(X\bar{X})} &= \sigma_{GF} \frac{\Gamma(\sigma \rightarrow X\bar{X})}{\Gamma_\sigma} \\
&\simeq \eta_{X\bar{X}} \sigma_{GF,SM}^{(X\bar{X})} \left\{ 1 + O\left(1 - \frac{\Gamma(\sigma \rightarrow b\bar{b})}{\Gamma_\sigma}\right) \right\} \\
&\simeq \eta_{X\bar{X}} \sigma_{GF,SM}^{(X\bar{X})},
\end{aligned} \tag{6}$$

where by  $\sigma_{GF,SM}^{(X\bar{X})}$  is meant the Gluon Fusion (GF) cross-section for a SM Higgs decaying into  $X\bar{X}$ . The last line follows from the fact that the dilaton decay width, like that of the Higgs, is dominated by the  $b\bar{b}$  final state.

The final states most sensitive to a Higgs-like dilaton produced through gluon fusion are  $\gamma\gamma$ ,  $WW^*$  and  $ZZ^*$ . These processes are insensitive to  $\epsilon$ , but depend on  $\xi$ , and in the case of the  $\gamma\gamma$  final state, also on  $\phi$ . The effect of  $\epsilon$  in the total width is largely cancelled by the enhancement in the coupling to the top that generates the coupling of the dilaton to the gluons. The fact that the observed rate to  $ZZ^*$  is comparable to that of the SM Higgs suggests that in this scenario values of  $\xi$  very different from unity are disfavored.

A similar analysis for the Vector Boson Fusion (VBF) and Associated Production (AP) modes leads to

$$\begin{aligned}
\sigma_{VBF,AP}^{(X\bar{X})} &= \sigma_{VBF,AP} \frac{\Gamma(\sigma \rightarrow X\bar{X})}{\Gamma_\sigma} \\
&\simeq \xi \frac{\eta_{X\bar{X}}}{\eta_{b\bar{b}}} \sigma_{VBF,AP,SM}^{(X\bar{X})}.
\end{aligned} \tag{7}$$

We see that in contrast to gluon fusion, the rates of VBF and AP processes do depend on  $\epsilon$ , except in the case of the  $b\bar{b}$  and  $\tau^+\tau^-$  final states.

To isolate the effect of  $\epsilon$  it is useful to take the ratio of GF and VBF (or AP)



rates to the same final state for the dilaton, and for the SM Higgs. Then,

$$\frac{\sigma_{GF}^{(X\bar{X})}/\sigma_{GF,SM}^{(X\bar{X})}}{\sigma_{VBF,AP}^{(X\bar{X})}/\sigma_{VBF,AP,SM}^{(X\bar{X})}} = (1 + \epsilon)^2 . \quad (8)$$

We remark that, especially for the measurement of a small  $\epsilon$ , it might be relevant to include higher-order corrections to the couplings under study, which, in general, make this ratio a function of all the modified couplings of this scenario.

We see from this analysis that the parameters  $\xi$ ,  $\epsilon$  and  $\phi$  can all be independently determined by combining different channels.

### 3.1.2 Composite Fermions

For composite SM fermions the parameter  $\psi$  replaces  $\epsilon$  in the parametrization of the coupling of the dilaton to the gluons. We first consider the case of dilatons produced through gluon fusion,

$$\sigma_{GF}^{(X\bar{X})} \simeq \eta_{X\bar{X}} \psi \sigma_{GF,SM}^{(X\bar{X})} . \quad (9)$$

We see that the rates to  $\gamma\gamma$ ,  $WW^*$  and  $ZZ^*$  now depend on both  $\psi$  and  $\xi$ , and in the case of  $\gamma\gamma$  on  $\phi$  as well.

For dilatons produced through vector boson fusion or associated production, we have

$$\sigma_{VBF,AP}^{(X\bar{X})} \simeq \eta_{X\bar{X}} \sigma_{VBF,AP,SM}^{(X\bar{X})} . \quad (10)$$

It follows that the VBF and AP modes are sensitive to  $\xi$ , but not to  $\psi$ .

In analogy with Eq. (8), one can isolate the effect of  $\psi$  by taking the ratio

$$\frac{\sigma_{GF}^{(X\bar{X})}/\sigma_{GF,SM}^{(X\bar{X})}}{\sigma_{VBF,AP}^{(X\bar{X})}/\sigma_{VBF,AP,SM}^{(X\bar{X})}} = \psi . \quad (11)$$

Once again we see that the parameters  $\xi$ ,  $\phi$  and  $\psi$  can all be independently

determined by appropriately combining the results of different channels.

### 3.2 Distinguishing Elementary and Composite Fermions

The scenarios with composite and elementary fermions correspond to very different theories in the ultraviolet (UV). Despite these stark differences in the UV distinguishing them on the basis of low energy observations might not be simple. For instance the couplings of the dilaton to gluons in the two scenarios are related by a change of parameters

$$\psi \leftrightarrow (1 + \epsilon)^2. \quad (12)$$

As the coupling to vector boson is the same it follows that from the study of the production cross-sections in the gluon fusion and vector boson fusion modes we cannot distinguish the two scenarios <sup>1</sup>. Some more information might be obtained by studying the (rare) production in association with  $t$  or  $b$  quarks or by adding to the analysis the information from the decay rates.

The key quantity to distinguish the two scenarios is the ratio

$$\eta_{gg}/\eta_{bb} \quad \text{or} \quad \eta_{gg}/\eta_{\tau\tau},$$

which is unity <sup>2</sup> in the elementary top scenario and a free parameter in the composite top scenario. To extract this quantity we can take the ratio of two generic  $GF$  and  $VBF$  (or  $AP$ ) modes  $X\bar{X}$  and  $Y\bar{Y}$  in units of the SM rates

$$\frac{\sigma_{GF}^{(X\bar{X})}/\sigma_{GF,SM}^{(X\bar{X})}}{\sigma_{VBF,AP}^{(Y\bar{Y})}/\sigma_{VBF,AP,SM}^{(Y\bar{Y})}} = \frac{\eta_{X\bar{X}}}{\eta_{Y\bar{Y}}} \frac{\eta_{gg}}{\eta_{WW}} \quad (13)$$

---

<sup>1</sup>The only restriction that applies in the relation Eq. (12) is that  $\epsilon > 0$ , hence when  $\psi < 1$  the scenario with elementary fermions cannot be mapped onto the composite fermions scenario.

<sup>2</sup>Strictly speaking  $\eta_{gg}/\eta_{bb}$  is one in the elementary fermions scenario only at tree-level. Going to higher order it becomes a function of all the other parameters. Furthermore both QCD and EW corrections should be included. In general it remains true that for the elementary fermions this ratio is predictable and fixed in terms of the other parameters, which makes the scenario distinguishable from the case with composite fermions.

and focus on the case  $X\bar{X} = WW$ ,  $Y\bar{Y} = b\bar{b}$  to obtain

$$\frac{\sigma_{GF}^{(WW)}/\sigma_{GF,SM}^{(WW)}}{\sigma_{VBF,AP}^{(bb)}/\sigma_{VBF,AP,SM}^{(bb)}} = \frac{\eta_{gg}}{\eta_{bb}}. \quad (14)$$

Analogously one can study the  $\tau^+\tau^-$  final state to get further information.

At the present time the errors on the measurements are still too large to draw conclusions on the value of this ratio. However we remark that both ATLAS and CMS reported measurements of the cross-sections involved, steadily improving their results. As such if the dilaton interpretation of the 125 GeV boson will turn out to be more appropriate than the one in terms of a SM Higgs boson, there is a chance that the measured cross-sections will provide a handle on the presence of colored states in the CFT in the UV.

### 3.3 Experimental data

The LHC and TeVatron experiments have searched for Higgs-like particles in a variety of final states. The data analyzed so far exhibits significant excesses over the expectation for the SM background. Striking evidence for a new boson has conclusively emerged from several analyses [88, 89].

While these observations still need to be refined the picture that has emerged seems to point towards new physics associated with a narrow resonance of mass about 125 GeV. As such the experiments tried to test an interpretation of the new boson in terms of a SM Higgs boson. To do that, for each relevant searched production and decay mode they presented the best fit value of the *signal strength* of a SM Higgs boson

$$\bar{\mu}_p^{(d)} = \frac{\sigma_{\text{best-fit}}}{\sigma_{p,SM}^{(d)}},$$

where  $d$  denotes the inclusive or exclusive final state searched for, and  $p = \text{inclusive, } GF, VBF, AP$  denotes the production mode of the SM Higgs.

For some final states, as for instance  $\gamma\gamma$ , the experiments find excesses even

compared to the expectations from a SM Higgs. These excesses are not statistically significant, but they nonetheless motivated further investigations of the 2011 and 2012 data in terms of various models of new physics. To increase their sensitivity to new physics both ATLAS and CMS performed a search for Higgs-like resonances in *exclusive* final states.

To isolate exclusive final states the dedicated Higgs searches require tags of special kinds of events, such as the presence of two energetic forward jet with large rapidity separation and very little hadronic activity in the central part of the detector. This configuration of QCD radiation accompanying the Higgs is typical of the VBF production mode, and therefore the “dijet” tag searches are essentially probes of the VBF production of the Higgs. Furthermore the experiments presented searches for the Higgs boson produced in association with a gauge boson, that are sensitive to different kinematical regions, but probe the same couplings as in VBF.

All the data presented by the experiments for Higgs searches can be translated into searches for the dilaton. In what follows we shall study how well the various dilaton scenarios fit the current data. We shall also try to see if in the current data one can spot the first hints of a preference for some of the scenarios of compositeness and EWSB described above.

As reference values for the SM Higgs properties we take the central values reported in [90, 91, 92] and summarized in Tables 2 and 3. For the convenience of the reader and to complete the description of our input data, in Table 4 we collect the best-fit signal strength  $\bar{\mu}_{p,d} \pm \delta\bar{\mu}_{p,d}$  used in our analysis.

When not specified the searches have been interpreted as inclusive searches, dominated by the GF production mechanism, but with the VBF and AP subdominant contributions taken into account. For both ATLAS and CMS data the signal strengths for the inclusive  $\gamma\gamma$  final state are computed combining in quadrature the relevant untagged di-photon categories. We checked that for a global com-

$BR(h \rightarrow XX)$					
$bb$	0.58				
$WW$	0.216				
$gg$	0.085				
$\tau\tau$	0.064				
$c\bar{c}$	0.0291				
$ZZ$	0.027				
$\gamma\gamma$	0.00228				
$Z\gamma$	0.00154				
$\mu\bar{\mu}$	0.00022				

$\sigma$ [pb]			
	LHC 8 TeV	LHC 7 TeV	TeVatron 1.96 TeV
GF	19.5	15.3	0.949
VBF	1.56	1.21	0.0653
WH	0.697	0.573	0.129
ZH	0.394	0.316	0.0785

Table 2: Properties of the SM Higgs boson at 125 GeV from [90, 91, 92].

$BR(h \rightarrow XX)$				
$bb$	0.553			
$WW$	0.239			
$gg$	0.0842			
$\tau\tau$	0.0608			
$c\bar{c}$	0.0279			
$ZZ$	0.0302			
$\gamma\gamma$	0.00228			
$Z\gamma$	0.00163			
$\mu\bar{\mu}$	0.000211			

$\sigma$ [pb]		
	LHC 8 TeV	LHC 7 TeV
GF	19.07	14.96
VBF	1.54	1.19
WH	0.669	0.550
ZH	0.379	0.304

Table 3: Properties of the SM Higgs boson at 126.5 GeV from [90, 91].

ATLAS $\tau\tau$ 2011	$0.2 \pm 1.8$
ATLAS bb AP 2011	$0.5 \pm 2.$
ATLAS WW 2011+2012	$1.4 \pm 0.5$
ATLAS ZZ 2011+2012	$1.3 \pm 0.6$
ATLAS $\gamma\gamma$ 2011+2012	$1.4 \pm 0.5$
ATLAS $\gamma\gamma$ dijet 2011	$2.7 \pm 1.8$
ATLAS $\gamma\gamma$ dijet 2012	$2.6 \pm 1.7$
CMS WW VBF 2011+2012	$0.2 \pm 1.5$
CMS $\gamma\gamma$ Dijet Loose 2012	$-0.6 \pm 2.$
CMS $\gamma\gamma$ Dijet Tight 2012	$1.3 \pm 1.6$
CMS $\gamma\gamma$ Dijet 2011	$4.2 \pm 2.$
CMS WW AP 2011	$-2.8 \pm 3.$
CMS $\tau\tau$ 2011+2012	$-0.2 \pm 0.8$
CMS bb AP 2011+2012	$0.5 \pm 0.8$
CMS WW 2011+2012	$0.6 \pm 0.4$
CMS ZZ 2011+2012	$0.8 \pm 0.4$
CMS $\gamma\gamma$ 2011+2012	$1.35 \pm 0.44$
TeVatron $\gamma\gamma$	$3.6 \pm 2.8$
TeVatron WW	$0.3 \pm 1.1$
TeVatron bb AP	$2. \pm 0.7$

Table 4: Signal strength best-fits extracted from [88, 89, 92, 93, 94, 95, 96, 97, 98]. AP stands for associated production. We take the best-fit signal strength for  $m_h = 125$  GeV throughout but for the  $\gamma\gamma$  searches of ATLAS where we take values at  $m_h=126.5$  GeV.

combination of all the the  $\gamma\gamma$  data the combination in quadrature reproduces the combination from the experiments within 10-20%. The associated production searches are explicitly marked as AP and are considered as pure associated production. The VBF searches have different degree of contamination from the GF process with emissions of extra-jets. In our analysis the VBF searches are all in the  $\gamma\gamma$  channel and we use the gluon fusion contamination reported in [93, 96]. We discard the information about searches in exclusive channels where we were not able to reconstruct the gluon-fusion contamination from the the public data. This is the case of the ‘‘CMS WW VBF 2011+2012’’ search reported by CMS.

As a check of the reliability of our treatment of the experimental data we reproduced the analysis of CMS for a Beyond the Standard Model (BSM) scenario with modified Higgs couplings to fermions and vectors. We observe rather good agreement with the result shown in [89] in the plane  $(c_V, c_F)$  (see Ref. [89] for a definition of these couplings).

### 3.4 Results

In this section we shall examine the 2011 and 2012 data from ATLAS, CMS and the TeVatron to assess whether the discovered boson at about 125 GeV is compatible with the properties of the general dilaton described above. In particular we shall determine what the current data tells us about the dynamics that underlies EWSB and the nature of the SM fermions in a dilaton scenario. We shall also discuss what observations can be done to cross-check the predictions of the different dilaton frameworks.

For each scenario we shall compute the minimum over the relevant parameters of the  $\chi^2$  between the observed data best-fit signal strengths  $\bar{\mu}_{p,d} \pm \delta\bar{\mu}_{p,d}$  of Table 4 and theory predictions  $\mu_{p,d}$  for the the signal strengths

$$\chi^2 = \sum_{i=\{(p,d)\}} \frac{(\bar{\mu}_i - \mu_i)^2}{\delta\bar{\mu}_i^2}, \quad (15)$$

where  $i$  runs over all the combinations of production modes  $p$  and decays  $d$  listed in Table 4.

As a reference for the analysis of the dilaton scenarios we compute the  $\chi^2$  for the SM Higgs boson. We obtain  $\chi^2 = 16.9$ . As we have a total of 19 measurements the SM seems in reasonable agreement with the current data.

### 3.5 Elementary fermions

In what follows we shall perform a fit of the available data using the coupling structure of a scenario with the elementary top. While we shall consider a fairly large range of  $\epsilon$ , our primary focus will be on the region  $0.35 \leq \epsilon \leq 0.55$ . The upper limit on the preferred range originates from the need to suppress potentially dangerous effects in flavor physics with a scale not too far below 1000 TeV, while the lower limit arises from the requirement that the CFT is a strongly coupled theory with significant anomalous dimensions, so that electroweak symmetry breaking is not overly fine tuned.

For the parameter  $\xi$  we restrict the best-fit to lie in the range  $0 \leq \xi \leq 2$ . This range is suitable for a generic scenario that encompasses both  $\xi$  values typical of a pNGB-like and technicolor-like mechanism for EWSB. The best fit parameters for this scenario are

$$\xi = 0.86, \epsilon = 0., \phi = 1.8, \tag{16}$$

which yields  $\chi^2 = 12.9$ . Imposing  $\epsilon \geq 0.35$  we get  $\chi^2 = 16.9$  for a best fit point

$$\xi = 0.68, \epsilon = 0.35, \phi = 2.2.$$

As we have 3 parameters for the couplings and a total of 19 measurements, the elementary top scenario seems in reasonable agreement with the current data for either choice of the minimal  $\epsilon$ .

Considering separately the measurements of ATLAS and CMS we obtain a



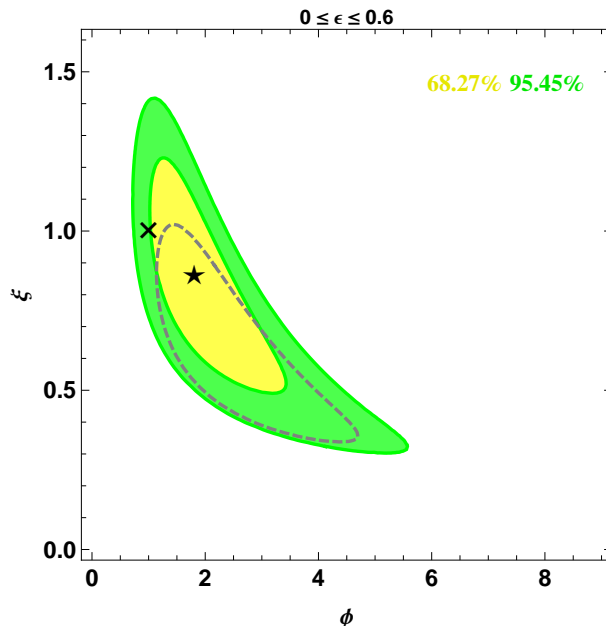


Figure 1: The  $1\sigma$  (yellow) and  $2\sigma$  (green) CL regions of the plane  $(\phi, \xi)$ . At each point the  $\chi^2$  has been minimized w.r.t.  $\epsilon$  in the range  $0 \leq \epsilon \leq 0.6$ . The black star corresponds to the best-fit point and the black cross is the location of the SM-Higgs-like dilaton. The dashed line corresponds to the  $2\sigma$  contour applying the further constraint  $\epsilon \geq 0.35$

result very similar to the global one for CMS, while ATLAS tends to prefer larger  $\xi$ , due to the larger rates in  $WW$  and  $ZZ$  modes.

To visualize the global constraint on  $\xi$  in Figure 1 we show the the  $1\sigma$  and  $2\sigma$  CL regions of the  $\chi^2$  minimized w.r.t  $\epsilon$  in the plane  $(\phi, \xi)$ . The current data prefers rather large values of  $\xi$ , in the domain of technicolor-like models. However pNGB-like values of  $\xi \sim 0.3$  are still allowed within  $2\sigma$ .

We remark that in the minimization on  $\epsilon$  performed in Figure 1 the value of  $\epsilon$  tends to hit the lower boundary of the imposed range. As explained in the discussion that lead to Eq. (8), the value of  $\epsilon$  is largely determined by the rates of the VBF and GF production modes. In the current data the most precise measurements are those in  $\gamma\gamma$  and the GF-dominated channels do not exhibit a larger excess than VBF. As a consequence  $\epsilon$  is driven to the minimal allowed value.

The strength of this pull can be visualized in Figure 2 where we show the

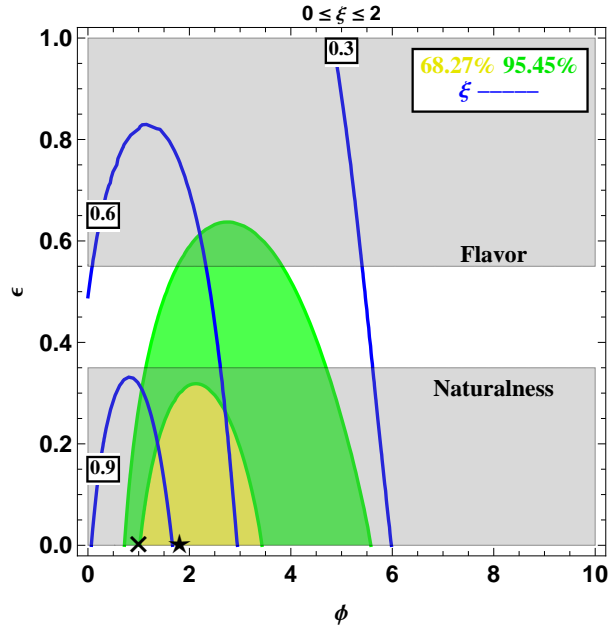


Figure 2: The  $1\sigma$  (yellow) and  $2\sigma$  (green) CL regions of the  $(\phi, \epsilon)$  plane. In each point the  $\chi^2$  is minimized w.r.t  $\xi$  in the interval  $0 \leq \xi \leq 2$ . The solid blue lines are the isolines of the value of  $\xi$  that minimizes the  $\chi^2$ . The black star corresponds to the best-fit point and the black cross is the location of the SM-Higgs-like dilaton. The upper gray-shaded region is disfavored by constraints from flavor physics. The lower gray-shaded region is disfavored by the bounds on the dimension of the operator  $\mathcal{H}^\dagger \mathcal{H}$  and their implications for the solution of the hierarchy problem discussed in Section 2.2.3.

$1\sigma$  and  $2\sigma$  CL regions of the plane  $(\phi, \epsilon)$ . The figure shows that in the region corresponding to large  $\xi$  points with big values of  $\epsilon$ , beyond  $\epsilon = 0.4$ , are still allowed within the the  $1\sigma$  CL region. In the pNGB-like region, that approximately lies close to and to the right of the isoline  $\xi = 0.3$ , we remark that the current data tends to push  $\epsilon$  towards zero, implying that this scenario is finetuned. It will be interesting to see how these constraints on  $\epsilon$  will evolve when further data becomes available, especially on the ratio  $\sigma_{VBF}^{(\gamma\gamma)}/\sigma_{GF}^{(\gamma\gamma)}$ .

### 3.6 Composite fermions

As in the case of the elementary top scenario for the parameter  $\xi$  we again consider a generic range  $0 \leq \xi \leq 2$ . The best fit parameters for this scenario are

$$\xi = 1.2, \psi = 0.59, \phi = 1.87,$$

which gives  $\chi^2 = 11.9$ . The composite top scenario seems in a reasonable agreement with the current data. Just as in the case of elementary top we observe that ATLAS data prefers larger values of  $\xi$ .

We remark that the preferred values of  $\psi$  are somewhat low. In particular at the best fit point the coupling of the gluons to the dilaton is suppressed with respect to the coupling of the Higgs in the SM. This is rather at odds with what we would expect from a CFT that contains colored states.

The tendency of the data to push  $\psi$  toward low values can be understood through Eq. (11). Analogously to what happens for  $\epsilon$  in the elementary top scenario,  $\psi$  is mostly determined by the ratio of VBF and GF rates and, due to the precision of the data, the  $\gamma\gamma$  final state has the stronger pull.

The strength of the pull on  $\psi$  is displayed in Figure 3 where we show the  $1\sigma$  and  $2\sigma$  CL regions of the plane  $(\phi, \psi)$  under the generic scenario for EWSB  $0 \leq \xi \leq 2$ . The figure shows that with small variations in  $\xi$  it is possible to have  $\psi \gtrsim 1$  within the  $2\sigma$  CL region indicated by the current data. We remark that the values of  $\psi$  and  $\phi$  in Eq. (5) for the scenario of composite massless gauge boson lie outside of the  $2\sigma$  CL region of the fit in our three parameter space. For completeness we report that the best fit for the scenario of composite massless gauge boson is  $\xi = 0.07$  which corresponds to  $\chi^2 = 21.6$ .

Furthermore we show in Figure 4 the  $1\sigma$  and  $2\sigma$  CL regions in the  $(\phi, \xi)$  plane together with the contours for the best-fit value of  $\psi$ . This figure makes explicit that reducing  $\xi$  from its best-fit value it is possible to accommodate points in the composite fermion parameter space with  $\psi \gtrsim 1$  within the  $2\sigma$  CL region.

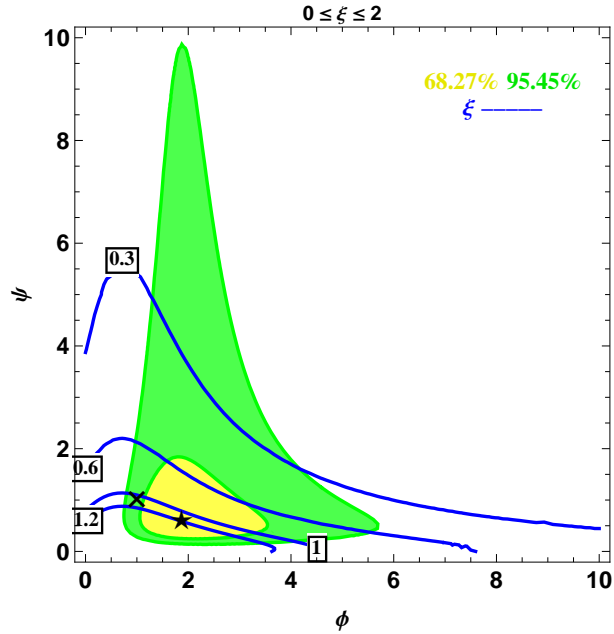


Figure 3: The  $1\sigma$  (yellow) and  $2\sigma$  (green) CL regions of the  $(\phi, \psi)$  plane. In each point the  $\chi^2$  is minimized w.r.t  $\xi$  in the interval  $0 \leq \xi \leq 2$ . The solid blue lines are the isolines of the value of  $\xi$  that minimizes the  $\chi^2$ . The black star corresponds to the best-fit point. The black cross is the location of the SM-Higgs-like dilaton.

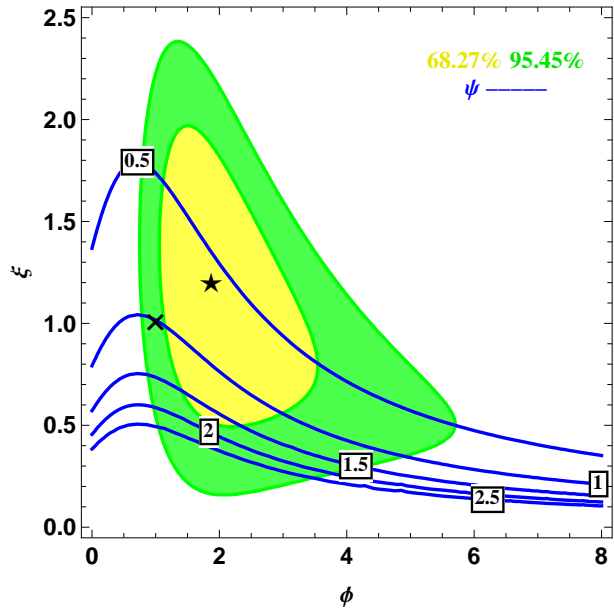


Figure 4: The  $1\sigma$  (yellow) and  $2\sigma$  (green) CL regions of the  $(\phi, \xi)$  plane. In each point the  $\chi^2$  is minimized w.r.t  $\psi$ . The solid blue lines are the isolines of the value of  $\psi$  that minimizes the  $\chi^2$ . The black star corresponds to the best-fit point. The black cross is the location of the SM-Higgs-like dilaton.

## 4 Conclusions

In this paper we have studied in detail the possibility that the 125 GeV resonance observed at CERN is the dilaton associated with the spontaneous breaking of an approximate conformal symmetry. Our focus has been on theories where this conformal dynamics underlies the breaking of electroweak symmetry. The discussion has been mostly carried on in a language suitable to describe at the same time scenarios where there is a pNGB Higgs boson that is relatively heavy and therefore yet to be discovered, as well as scenarios where the breaking of the EW symmetry arises directly from strong dynamics as in technicolor models.

We have considered a rather wide spectrum of possibilities for the properties of the known SM states within the dilaton framework. In particular, we have allowed for both elementary and composite fermions. Furthermore we have considered both the case when the SM gauge bosons are composites of the CFT and the case when they are elementary states.

We have discussed how the LHC Higgs data can be used to investigate the realization of all these scenarios for the dilaton. In particular we have introduced an effective description of the coupling structure that is suitable to take into account the leading order physics of the interactions of the dilaton with the SM states. The adopted parametrization naturally accommodates the effects of the breaking of conformal symmetry on the couplings of the dilaton. The summary of the coupling structure we have considered is reported in Table 1. We stress that this parametrization exhibits wide coverage; for instance it captures dilatons from RS constructions with different embeddings of the fermions as well as dilatons for which there is no known corresponding RS realization.

Motivated by the impressive results of the experiments at the LHC, we have studied the specific measurements that are critical to uncovering the nature of the dilaton that could be responsible for the signal at 125 GeV. For this it was essential to exploit the capabilities that the experiments have demonstrated in

disentangling the several exclusive channels that contribute to the data about the 125 GeV resonance. We have shown that using this information it is also possible to address questions about the elementary or composite nature of the SM fermions and gauge bosons.

We have confronted the several possible incarnations of the dilaton against the set of available measurements in Higgs searches. We have identified the regions of the parameter space that are favored by the current measurements, and find that it is generically preferred to have a dilaton whose couplings resemble rather closely those of SM Higgs boson. Although we find that the coupling structure of the dilaton does in principle allow better agreement with the central values of the current measurements than the SM Higgs, the uncertainties are at the moment sufficiently large that from a global  $\chi^2$  analysis a statistically significant preference does not emerge. Since further data from the 2012 run of the LHC may begin to highlight significant deviations from the predictions of a SM Higgs, we believe that it is worth considering the dilaton, in its full generality, as a potential explanation of the new physics at 125 GeV.

## Acknowledgements

We are glad to thank Christophe Grojean and David Poland for discussions and comments on our manuscript. RF also thanks Roberto Contino and Alessandro Strumia for important discussions. This work is supported by the NSF under grant PHY-0968854. The work of RF is supported by the NSF Grants PHY-0910467 and by the Maryland Center for Fundamental Physics. RF thanks CERN TH division for hospitality and support while this work was completed. RF acknowledges the hospitality of the Aspen Center for Physics, which is supported by the NSF Grant No. PHY-1066293.

**Note added:** While we were completing this paper, we were informed of the upcoming work [99] which overlaps with some of the ideas presented here.

## References

- [1] The CMS Collaboration, “Observation of a new boson at a mass of 125 GeV with the CMS experiment at the LHC,” *ArXiv e-prints* (July, 2012) , [arXiv:1207.7235 \[hep-ex\]](#). [WEBSITE](#).
- [2] The ATLAS Collaboration, “Observation of a new particle in the search for the Standard Model Higgs boson with the ATLAS detector at the LHC,” *ArXiv e-prints* (July, 2012) , [arXiv:1207.7214 \[hep-ex\]](#). [WEBSITE](#).
- [3] D. Carmi, A. Falkowski, E. Kuflik, and T. Volansky, “Interpreting LHC Higgs Results from Natural New Physics Perspective,” *ArXiv e-prints* (Feb., 2012) , [arXiv:1202.3144 \[hep-ph\]](#).
- [4] A. Azatov, R. Contino, and J. Galloway, “Model-Independent Bounds on a Light Higgs,” *ArXiv e-prints* (Feb., 2012) , [arXiv:1202.3415 \[hep-ph\]](#).
- [5] J. R. Espinosa, C. Grojean, M. Muhlleitner, and M. Trott, “Fingerprinting Higgs Suspects at the LHC,” *ArXiv e-prints* (Feb., 2012) , [arXiv:1202.3697 \[hep-ph\]](#).
- [6] P. P. Giardino, K. Kannike, M. Raidal, and A. Strumia, “Reconstructing Higgs boson properties from the LHC and Tevatron data,” *ArXiv e-prints* (Mar., 2012) , [arXiv:1203.4254 \[hep-ph\]](#).
- [7] J. Ellis and T. You, “Global Analysis of Experimental Constraints on a Possible Higgs-Like Particle with Mass  $\sim 125$  GeV,” *ArXiv e-prints* (Apr., 2012) , [arXiv:1204.0464 \[hep-ph\]](#).
- [8] M. Klute, R. Lafaye, T. Plehn, M. Rauch, and D. Zerwas, “Measuring Higgs Couplings from LHC Data,” *ArXiv e-prints* (May, 2012) , [arXiv:1205.2699 \[hep-ph\]](#).



- [9] T. Corbett, O. J. P. Eboli, J. Gonzalez-Fraile, and M. C. Gonzalez-Garcia, “Constraining anomalous Higgs interactions,” *ArXiv e-prints* (July, 2012) , [arXiv:1207.1344 \[hep-ph\]](#).
- [10] P. P. Giardino, K. Kannike, M. Raidal, and A. Strumia, “Is the resonance at 125 GeV the Higgs boson?,” *ArXiv e-prints* (July, 2012) , [arXiv:1207.1347 \[hep-ph\]](#).
- [11] D. Carmi, A. Falkowski, E. Kuflik, T. Volansky, and J. Zupan, “Higgs After the Discovery: A Status Report,” *ArXiv e-prints* (July, 2012) , [arXiv:1207.1718 \[hep-ph\]](#).
- [12] J. R. Espinosa, C. Grojean, M. Muhlleitner, and M. Trott, “First Glimpses at Higgs’ face,” *ArXiv e-prints* (July, 2012) , [arXiv:1207.1717 \[hep-ph\]](#).
- [13] J. Ellis and T. You, “Global Analysis of the Higgs Candidate with Mass  $\sim 125$  GeV,” *ArXiv e-prints* (July, 2012) , [arXiv:1207.1693 \[hep-ph\]](#).
- [14] I. Low, J. Lykken, and G. Shaughnessy, “Have We Observed the Higgs (Imposter)?,” *ArXiv e-prints* (July, 2012) , [arXiv:1207.1093 \[hep-ph\]](#).
- [15] M. Montull and F. Riva, “Higgs discovery: the beginning or the end of natural EWSB?,” *ArXiv e-prints* (July, 2012) , [arXiv:1207.1716 \[hep-ph\]](#).
- [16] M. R. Buckley and D. Hooper, “Are There Hints of Light Stops in Recent Higgs Search Results?,” *ArXiv e-prints* (July, 2012) , [arXiv:1207.1445 \[hep-ph\]](#).
- [17] J. F. Gunion, Y. Jiang, and S. Kraml, “Could two NMSSM Higgs bosons be present near 125 GeV?,” *ArXiv e-prints* (July, 2012) , [arXiv:1207.1545 \[hep-ph\]](#).

- [18] E. Gabrielli, K. Kannike, B. Mele, A. Racioppi, and M. Raidal, “Fermiophobic Higgs boson and supersymmetry,” *ArXiv e-prints* (Mar., 2012) , [arXiv:1204.0080 \[hep-ph\]](#).
- [19] E. Gabrielli, B. Mele, and M. Raidal, “Has a fermiophobic Higgs boson been detected at the LHC?,” *ArXiv e-prints* (Feb., 2012) , [arXiv:1202.1796 \[hep-ph\]](#).
- [20] J. R. Espinosa, M. Muhlleitner, C. Grojean, and M. Trott, “Probing for Invisible Higgs Decays with Global Fits,” *ArXiv e-prints* (May, 2012) , [arXiv:1205.6790 \[hep-ph\]](#).
- [21] H. K. Dreiner, J. S. Kim, and O. Lebedev, “First LHC Constraints on Neutralinos,” *ArXiv e-prints* (June, 2012) , [arXiv:1206.3096 \[hep-ph\]](#).
- [22] A. Azatov, R. Contino, D. Del Re, J. Galloway, M. Grassi, and S. Rahatlou, “Determining Higgs couplings with a model-independent analysis of  $h \rightarrow \gamma\gamma$ ,” *ArXiv e-prints* (Apr., 2012) , [arXiv:1204.4817 \[hep-ph\]](#).
- [23] Kraml, S. et al., “Searches for new physics: Les Houches recommendations for the presentation of LHC results,” *European Physical Journal C* **72** (Apr., 2012) 1976, [arXiv:1203.2489 \[hep-ph\]](#).
- [24] L. Susskind, “Dynamics of Spontaneous Symmetry Breaking in the Weinberg-Salam Theory,” *Phys.Rev.* **D20** (1979) 2619–2625.
- [25] S. Weinberg, “Implications of Dynamical Symmetry Breaking,” *Phys.Rev.* **D13** (1976) 974–996.
- [26] C. T. Hill and E. H. Simmons, “Strong dynamics and electroweak symmetry breaking,” *Phys.Rept.* **381** (2003) 235–402, [arXiv:hep-ph/0203079 \[hep-ph\]](#).

- [27] H. Georgi and A. Pais, “Calculability and Naturalness in Gauge Theories,” *Phys.Rev.* **D10** (1974) 539.
- [28] H. Georgi and A. Pais, “Vacuum Symmetry and the PseudoGoldstone Phenomenon,” *Phys.Rev.* **D12** (1975) 508.
- [29] D. B. Kaplan and H. Georgi, “SU(2) x U(1) Breaking by Vacuum Misalignment,” *Phys.Lett.* **B136** (1984) 183.
- [30] D. B. Kaplan, H. Georgi, and S. Dimopoulos, “Composite Higgs Scalars,” *Phys.Lett.* **B136** (1984) 187.
- [31] H. Georgi and D. B. Kaplan, “Composite Higgs and Custodial SU(2),” *Phys.Lett.* **B145** (1984) 216.
- [32] M. A. Luty and T. Okui, “Conformal technicolor,” *Journal of High Energy Physics* **9** (Sept., 2006) 70, [arXiv:hep-ph/0409274](https://arxiv.org/abs/hep-ph/0409274).
- [33] B. Holdom, “Technicolor,” *Phys.Lett.* **B150** (1985) 301.
- [34] T. W. Appelquist, D. Karabali, and L. Wijewardhana, “Chiral Hierarchies and the Flavor Changing Neutral Current Problem in Technicolor,” *Phys.Rev.Lett.* **57** (1986) 957.
- [35] K. Yamawaki, M. Bando, and K.-i. Matumoto, “Scale Invariant Technicolor Model and a Technidilaton,” *Phys.Rev.Lett.* **56** (1986) 1335.
- [36] T. Appelquist and L. Wijewardhana, “Chiral Hierarchies and Chiral Perturbations in Technicolor,” *Phys.Rev.* **D35** (1987) 774.
- [37] T. Appelquist and L. Wijewardhana, “Chiral Hierarchies from Slowly Running Couplings in Technicolor Theories,” *Phys.Rev.* **D36** (1987) 568.
- [38] A. Salam and J. Strathdee, “Nonlinear realizations. 2. Conformal symmetry,” *Phys.Rev.* **184** (1969) 1760–1768.

- [39] C. Isham, A. Salam, and J. Strathdee, “Nonlinear realizations of space-time symmetries. Scalar and tensor gravity,” *Annals Phys.* **62** (1971) 98–119.
- [40] B. Zumino, “Lectures on Elementary Particles and Quantum Field Theory, edited by S. Deser *et. al.*, MIT Press (1970),” *1970 Brandeis Summer School*.
- [41] J. R. Ellis, “Aspects of conformal symmetry and chirality,” *Nucl.Phys.* **B22** (1970) 478–492.
- [42] R. Rattazzi and A. Zaffaroni, “Comments on the Holographic Picture of the Randall-Sundrum Model,” *Journal of High Energy Physics* **4** (Apr., 2001) 21, [arXiv:hep-th/0012248](#).
- [43] Goldberger, W.D. and Grinstein, B. and Skiba, W., “Distinguishing the Higgs Boson from the Dilaton at the Large Hadron Collider,” *Physical Review Letters* **100** no. 11, (Mar., 2008) 111802, [arXiv:0708.1463 \[hep-ph\]](#).
- [44] L. Vecchi, “Phenomenology of a light scalar: the dilaton,” *Phys.Rev.* **D82** (2010) 076009, [arXiv:1002.1721 \[hep-ph\]](#).
- [45] Z. Chacko and R. K. Mishra, “Effective theory of a light dilaton,” [arXiv:1209.3022 \[hep-ph\]](#).
- [46] J. Fan, W. D. Goldberger, A. Ross, and W. Skiba, “Standard Model couplings and collider signatures of a light scalar,” *Phys.Rev.* **D79** (2009) 035017, [arXiv:0803.2040 \[hep-ph\]](#).
- [47] B. Coleppa, T. Grégoire, and H. E. Logan, “Dilaton constraints and LHC prospects,” *Phys. Rev. D* **85** no. 5, (Mar., 2012) 055001, [arXiv:1111.3276 \[hep-ph\]](#).

- [48] B. A. Campbell, J. Ellis, and K. A. Olive, “Phenomenology and cosmology of an electroweak pseudo-dilaton and electroweak baryons,” *Journal of High Energy Physics* **3** (Mar., 2012) 26, [arXiv:1111.4495 \[hep-ph\]](#).
- [49] H. de Sandes and R. Rosenfeld, “Radion-Higgs mixing effects on bounds from LHC Higgs boson searches,” *Phys. Rev. D* **85** no. 5, (Mar., 2012) 053003, [arXiv:1111.2006 \[hep-ph\]](#).
- [50] V. Barger, M. Ishida, and W.-Y. Keung, “Differentiating the Higgs Boson from the Dilaton and Radion at Hadron Colliders,” *Physical Review Letters* **108** no. 10, (Mar., 2012) 101802, [arXiv:1111.4473 \[hep-ph\]](#).
- [51] V. Barger, M. Ishida, and W.-Y. Keung, “Dilaton at the LHC,” *Phys. Rev. D* **85** no. 1, (Jan., 2012) 015024, [arXiv:1111.2580 \[hep-ph\]](#).
- [52] D. Elander and M. Piai, “The decay constant of the holographic techni-dilaton and the 125 GeV boson,” *ArXiv e-prints* (Aug., 2012) , [arXiv:1208.0546 \[hep-ph\]](#).
- [53] S. Matsuzaki and K. Yamawaki, “Is 125 GeV techni-dilaton found at LHC?,” *ArXiv e-prints* (July, 2012) , [arXiv:1207.5911 \[hep-ph\]](#).
- [54] S. Matsuzaki and K. Yamawaki, “Discovering 125 GeV techni-dilaton at LHC,” *ArXiv e-prints* (June, 2012) , [arXiv:1206.6703 \[hep-ph\]](#).
- [55] S. Matsuzaki and K. Yamawaki, “Techni-dilaton at 125 GeV,” *ArXiv e-prints* (Jan., 2012) , [arXiv:1201.4722 \[hep-ph\]](#).
- [56] S. Matsuzaki and K. Yamawaki, “Holographic techni-dilaton at 125 GeV,” *ArXiv e-prints* (Sept., 2012) , [arXiv:1209.2017 \[hep-ph\]](#).
- [57] B. Grzadkowski, J. F. Gunion, and M. Toharia, “Higgs-radion interpretation of the LHC data?,” *Physics Letters B* **712** (May, 2012) 70–80, [arXiv:1202.5017 \[hep-ph\]](#).

- [58] K. Cheung and T.-C. Yuan, “Could the Excess Seen at 124-126 GeV Be due to the Randall-Sundrum Radion?,” *Physical Review Letters* **108** no. 14, (Apr., 2012) 141602, [arXiv:1112.4146 \[hep-ph\]](#).
- [59] J. Maldacena, “The Large-N Limit of Superconformal Field Theories and Supergravity,” *International Journal of Theoretical Physics* **38** (1999) 1113–1133, [arXiv:hep-th/9711200](#).
- [60] E. Witten, “Anti De Sitter Space And Holography,” *ArXiv High Energy Physics - Theory e-prints* (Feb., 1998) , [arXiv:hep-th/9802150](#).
- [61] H. Verlinde, “Holography and compactification,” *Nuclear Physics B* **580** (July, 2000) 264–274, [arXiv:hep-th/9906182](#).
- [62] E. Verlinde and H. Verlinde, “RG-flow, gravity and the cosmological constant,” *Journal of High Energy Physics* **5** (May, 2000) 34, [arXiv:hep-th/9912018](#).
- [63] L. Randall and R. Sundrum, “Large Mass Hierarchy from a Small Extra Dimension,” *Physical Review Letters* **83** (Oct., 1999) 3370–3373, [arXiv:hep-ph/9905221](#).
- [64] C. Csáki, C. Grojean, L. Pilo, and J. Terning, “Towards a Realistic Model of Higgsless Electroweak Symmetry Breaking,” *Physical Review Letters* **92** no. 10, (Mar., 2004) 101802, [arXiv:hep-ph/0308038](#).
- [65] R. Contino, Y. Nomura, and A. Pomarol, “Higgs as a holographic pseudo-Goldstone boson,” *Nuclear Physics B* **671** (Nov., 2003) 148–174, [arXiv:hep-ph/0306259](#).
- [66] K. Agashe, R. Contino, and A. Pomarol, “The minimal composite Higgs model,” *Nuclear Physics B* **719** (July, 2005) 165–187, [arXiv:hep-ph/0412089](#).

- [67] W. D. Goldberger and M. B. Wise, “Modulus stabilization with bulk fields,” *Phys.Rev.Lett.* **83** (1999) 4922–4925, [arXiv:hep-ph/9907447](#) [[hep-ph](#)].
- [68] C. Csaki, M. Graesser, L. Randall, and J. Terning, “Cosmology of brane models with radion stabilization,” *Phys. Rev. D* **62** no. 4, (Aug., 2000) 045015, [arXiv:hep-ph/9911406](#).
- [69] W. D. Goldberger and M. B. Wise, “Phenomenology of a stabilized modulus,” *Phys.Lett.* **B475** (2000) 275–279, [arXiv:hep-ph/9911457](#) [[hep-ph](#)].
- [70] G. F. Giudice, R. Rattazzi, and J. D. Wells, “Graviscalars from higher-dimensional metrics and curvature-Higgs mixing,” *Nuclear Physics B* **595** (Feb., 2001) 250–276, [arXiv:hep-ph/0002178](#).
- [71] C. Csaki, M. L. Graesser, and G. D. Kribs, “Radion dynamics and electroweak physics,” *Phys.Rev.* **D63** (2001) 065002, [arXiv:hep-th/0008151](#) [[hep-th](#)].
- [72] T. G. Rizzo, “Radion couplings to bulk fields in the Randall-Sundrum model,” *JHEP* **0206** (2002) 056, [arXiv:hep-ph/0205242](#) [[hep-ph](#)].
- [73] C. Csaki, J. Hubisz, and S. J. Lee, “Radion phenomenology in realistic warped space models,” *Phys.Rev.* **D76** (2007) 125015, [arXiv:0705.3844](#) [[hep-ph](#)].
- [74] C. Isham, A. Salam, and J. Strathdee, “Spontaneous breakdown of conformal symmetry,” *Phys.Lett.* **B31** (1970) 300–302.
- [75] J. R. Ellis, “Phenomenological actions for spontaneously-broken conformal symmetry,” *Nucl.Phys.* **B26** (1971) 536–546.
- [76] R. Rattazzi, “The naturally light dilaton,” *Talk at Planck 2010* .

- [77] T. Appelquist and Y. Bai, “A Light Dilaton in Walking Gauge Theories,” *Phys.Rev.* **D82** (2010) 071701, [arXiv:1006.4375 \[hep-ph\]](#).
- [78] Y. Tang, “Implications of LHC Searches for Massive Graviton,” *ArXiv e-prints* (June, 2012) , [arXiv:1206.6949 \[hep-ph\]](#).
- [79] Y. Tang, “Comment on "could the excess seen at 124-126 gev be due to the randall-sundrum radion?", *ArXiv e-prints* (April, 2012) , [arXiv:1204.6145 \[hep-ph\]](#).
- [80] R. Rattazzi, V. S. Rychkov, E. Tonni, and A. Vichi, “Bounding scalar operator dimensions in 4D CFT,” *Journal of High Energy Physics* **12** (Dec., 2008) 31, [arXiv:0807.0004 \[hep-th\]](#).
- [81] V. S. Rychkov and A. Vichi, “Universal Constraints on Conformal Operator Dimensions,” *Phys.Rev.* **D80** (2009) 045006, [arXiv:0905.2211 \[hep-th\]](#).
- [82] R. Rattazzi, S. Rychkov, and A. Vichi, “Bounds in 4D conformal field theories with global symmetry,” *Journal of Physics A Mathematical General* **44** no. 3, (Jan., 2011) 035402, [arXiv:1009.5985 \[hep-th\]](#).
- [83] A. Vichi, “Improved bounds for CFT’s with global symmetries,” *Journal of High Energy Physics* **1** (Jan., 2012) 162, [arXiv:1106.4037 \[hep-th\]](#).
- [84] D. Poland, D. Simmons-Duffin, and A. Vichi, “Carving Out the Space of 4D CFTs,” *JHEP* **1205** (2012) 110, [arXiv:1109.5176 \[hep-th\]](#).
- [85] D. Poland and D. Simmons-Duffin, “Bounds on 4D conformal and superconformal field theories,” *Journal of High Energy Physics* **5** (May, 2011) 17, [arXiv:1009.2087 \[hep-th\]](#).
- [86] D. B. Kaplan, “Flavor at SSC energies: A New mechanism for dynamically generated fermion masses,” *Nucl.Phys.* **B365** (1991) 259–278.



- [87] R. Contino, T. Kramer, M. Son, and R. Sundrum, “Warped/composite phenomenology simplified,” *JHEP* **0705** (2007) 074, [arXiv:hep-ph/0612180 \[hep-ph\]](#).
- [88] ATLAS Collaboration, “Observation of an Excess of Events in the Search for the Standard Model Higgs boson with the ATLAS detector at the LHC,” Tech. Rep. ATLAS-CONF-2012-093, CERN, Geneva, Jul, 2012. [WEBSITE](#).
- [89] CMS Collaboration, “Observation of a new boson with a mass near 125 GeV,” *CMS-PAS-HIG-12-020* (2012) . [WEBSITE](#).
- [90] LHC Higgs Cross Section Working Group, “Handbook of LHC Higgs Cross Sections: 1. Inclusive Observables,” *eprint arXiv:1101.0593* (Jan., 2011) , [arXiv:1101.0593 \[hep-ph\]](#).
- [91] “LHC Higgs Cross Section Working Group.” [WEBSITE](#).
- [92] The CDF Collaboration, the D0 Collaboration, t. Tevatron New Physics, and Higgs Working Group, “Updated Combination of CDF and D0 Searches for Standard Model Higgs Boson Production with up to 10.0 fb<sup>-1</sup> of Data,” *ArXiv e-prints* (July, 2012) , [arXiv:1207.0449 \[hep-ex\]](#).
- [93] CMS Collaboration, “Evidence for a new state decaying into two photons in the search for the standard model Higgs boson in pp collisions,” *CMS-PAS-HIG-12-015* (2012) . [WEBSITE](#).
- [94] CMS Collaboration, “Combination of SM, SM4, FP Higgs boson searches,” *CMS-PAS-HIG-12-008* (2012) . [WEBSITE](#).
- [95] ATLAS Collaboration, “Combined search for the Standard Model Higgs boson in pp collisions at  $\sqrt{s} = 7$  TeV with the ATLAS detector,” *ArXiv e-prints* (July, 2012) , [arXiv:1207.0319 \[hep-ex\]](#).

- [96] “Observation of an excess of events in the search for the Standard Model Higgs boson in the gamma-gamma channel with the ATLAS detector,” Tech. Rep. ATLAS-CONF-2012-091, CERN, Geneva, Jul, 2012. [WEBSITE](#).
- [97] ATLAS Collaboration, “Observation of an excess of events in the search for the Standard Model Higgs boson in the  $H \rightarrow ZZ^{(*)} \rightarrow 4\ell$  channel with the ATLAS detector,” Tech. Rep. ATLAS-CONF-2012-092, CERN, Geneva, Jul, 2012. [WEBSITE](#).
- [98] ATLAS Collaboration, “Observation of an Excess of Events in the Search for the Standard Model Higgs Boson in the  $H \rightarrow WW^{(*)} \rightarrow \ell\nu\ell\nu$  Channel with the ATLAS Detector,” Tech. Rep. ATLAS-CONF-2012-098, CERN, Geneva, Jul, 2012. [WEBSITE](#).
- [99] B. Bellazzini, C. Csáki, J. Hubisz, J. Serra, and J. Terning, “A Higgslike Dilaton,” *ArXiv e-prints* (Sept., 2012) , [arXiv:1209.3299 \[hep-ph\]](#).